Nonlinear calculation of stopping powers for protons and antiprotons in solids: The Barkas effect

N. R. Arista and A. F. Lifschitz
Centro Atómico Bariloche and Instituto Balseiro, Comisión Nacional de Energía Atómica, 8400 Bariloche, Argentina
(Received 6 July 1998; revised manuscript received 19 October 1998)

We calculate the electronic energy loss of protons and antiprotons in solids for a wide range of energies using a self-consistent method based on the extension of the Friedel sum rule to finite velocities. The calculations show the importance of nonlinear effects in the interaction of the moving particles with valence electrons in the intermediate range of energies around the stopping power maximum. The calculations give the magnitude and the velocity dependence of these effects, and provide a consistent theoretical explanation of recent experimental results for aluminum and silicon.
[S1050-2947(99)04903-3]

PACS number(s): 34.50.Bw, 34.50.Fa, 79.20.Rf

I. INTRODUCTION

The discovery of different penetration ranges for positive and negative pions in matter made by Barkas and co-workers [1] was the first evidence of deviations from the quadratic dependence on projectile charge Z, predicted by the Bethe theory of the stopping power of energetic particles [2]. The origin of this difference was already proposed by Barkas due to higher-order, or Z^3 terms, in the perturbative Born approximation. The first calculation of this so-called Barkas effect, was made by Ashley, Ritchie, and Brandt [3,4] and it was further studied by other authors [5,6]. More recent developments based on the quantum oscillator model [7–9] provide general scaling functions for the Z^2,Z^3, and Z^4 terms, respectively, which can be used to estimate the contributions from the different atomic shells. A quantitative analysis of the Barkas effect based on these previous models has been made by Bichsel [10].

Recent advances in experimental techniques have made it possible to obtain low-energy antiprotons with energies down to a few tens of keV's, and then to launch a set of investigations on interactions of protons and antiprotons with matter [11]. The most recent experiments provide valuable information on the p-$\bar{p}$ differences in the stopping powers for various solid elements at energies around and below the stopping power maximum [12,13]. This collection of data is of great interest to test theoretical models aiming to describe the Barkas effect, since the stopping power differences become very large in this energy range. However, the perturbative methods, which are useful at high energies, begin to fail near the stopping power maximum. We note in particular that the results from the perturbative expansions predict a behavior of the Z^3 term that increases to lower energies following a $(Z/v)^3$ dependence [3–6]. Therefore the usual perturbative expansion becomes questionable in the lower energy range.

On the other hand, using many-body techniques and the random-phase approximation, a formulation of the quadratic response function of a free electron gas has been recently developed [14]. This formulation provides the Z^2 and Z^3 terms in the perturbative expansion, showing also the dependence with ion velocity v. These results may be useful at high velocities or for small r_s values, where a perturbative picture can be constructed. But for slow protons and r_s values in the metallic range, the differences in the stopping powers, as compared with the more exact density-functional values, are too large [14].

Previous theoretical evaluations of the Barkas effect at low energies for the p-$\bar{p}$ case have been based on the nonperturbative (or nonlinear) framework of the density-functional theory (DFT) [15,16]. Other calculations have used trial potentials with appropriate parameters to represent nonlinear screening conditions [17–19]. The possibility to extend the DFT to the case of moving particles is still an open question; the main difficulties arise from the breakdown of the spherical symmetry of the dynamical potential, and the increasing range of the interactions due to the weakening screening conditions (which requires the inclusion of an increasing number of scattering terms). An intermediate approach may be to include the velocity-dependent terms in the momentum transfer equations, while keeping the scattering potential frozen (equal to the DFT potential for static particles), but this procedure yields too small stopping power values since the increasing range of the potential is not taken into account [18,20]. In a recent publication, Nagy and Apagyi have formulated a model based on quantum calculations of transport cross sections for velocity-dependent potentials, averaging over the nonhomogeneous electron density distribution to include the contribution from inner shells [21].

Here we propose an alternative approach to this problem, which is based on an extension of the Friedel sum rule to finite velocities and a self-consistent optimization of the scattering potential and related phase shifts. The main assumption of the model lies in the spherical symmetry of the average potential, however the self-consistent method used in the optimization has been found to give very good results for the mean energy loss even at high velocities [22,23]. On the other hand, the main advantage of this model is that it may be solved in an exact quantum-mechanical way for any velocity of interest, and it provides a closed approach to calculate the nonlinear effects in the relevant range of intermedi-

ate velocities, i.e., around the stopping power maximum, which is usually the most complex range for stopping power calculations [24].

Using this approach we evaluate the energy losses of protons and antiprotons in aluminum and silicon, where the main contribution to the stopping power maximum is given by valence electrons. The calculations are compared with experimental results on the relevant range of energies, and provide clear evidence of the magnitude and velocity dependence of the nonlinear effects in this energy range.

II. MODEL

The generalization of the Friedel sum rule to finite velocities and the application to the energy loss problem were developed in Ref. [22], so we give here only a brief description. In the present context, the extended sum rule for a particle with velocity v may be written in the form

$$\frac{2}{\pi}\sum_{l=0}^{\infty}(2l+1)G_l(v,v_F)=Z_1, \tag{1}$$

where $Z_1=\pm 1$ for protons and antiprotons and v_F is the Fermi velocity of the solid. The function $G_l(v,v_F)$ takes into account the contribution of each l-wave component to the screening charge, and may be expressed as an integral of the phase shift contributions over a displaced Fermi sphere (DFS), as follows:

$$G_l(v,v_F)=\frac{1}{4\pi}\int_{\mathrm{DFS}}\left[\frac{d\delta_l(k)}{dk}\right]d\Omega\ \ dk$$
$$=\int_{k_{\min}}^{k_{\max}}\left[\frac{d\delta_l(k)}{dk}\right]g(k,v)dk, \tag{2}$$

where $k_{\min}=\max\{0,v-v_F\}$, $k_{\max}=v+v_F$; the function $g(k,v)$ takes into account the angular part of the integration over the DFS, and its value is given in Ref. [22] for the cases $v<v_F$ and $v>v_F$. $\delta_l(k)$ denotes the phase shifts of the electron wave function due to the scattering process, which is described in the center of mass system (coincident with the massive ion in the present approximation), and $[d\delta_l(k)/dk]$ gives the contribution of the l wave to the accumulation of screening charge. It may be shown from these expressions that one retrieves the usual Friedel sum rule in the low-velocity limit ($v<v_F$), and a perturbative form of the sum rule for high velocities ($v>v_F$) [22,25].

The scattering potential was assumed of the form of a simple screened potential, with a dynamical screening parameter α, whose value is adjusted in a self-consistent way according to the extended sum rule. In our previous calculations [22] we have considered in detail the results obtained using either a Yukawa or a hydrogenic form for the screened potential, and we have shown that a very good agreement is obtained in both cases for the whole range of r_s values of interest by comparing with the more exact results obtained by the density-functional theory, provided that the potential parameters are adjusted according to the Friedel sum rule. In particular, a very close agreement was obtained using a Yukawa type of potential (cf. Fig. 4 of Ref. [22]). Based on these results, we assumed here this form of screening function, with a screening parameter α which is adjusted for each ion velocity as follows: for each value of α, many phase shifts $\delta_l(k)$ are calculated by numerical integration of the Schrödinger equation, and then Eqs. (1) and (2) are used to evaluate the extended sum rule. These calculations are repeated by an iteration routine, varying the value of α until the sum rule (1) is satisfied. With increasing velocities the values of α decrease and the convergence of the partial-wave series becomes slower; for the largest velocities considered here (~ 10 a.u.) α becomes of the order of 0.05 a.u., and one should include up to 600 phase shifts to maintain a good precision in the results. However, for large values of l we have found it more convenient to use the semiclassical approximation to calculate the δ_l values [22]. The calculations with this method have been always straightforward, and no troubles in converging to the self-consistent solution have been found.

Once this self-consistent screening condition is achieved, the stopping power $S=\langle dE/dx\rangle$ is calculated using a former result [22,26] expressed in terms of the transport cross section σ_{tr}, namely (atomic units are used)

$$S_{\mathrm{valence}}=\frac{1}{4\pi^2v^2}\int_0^{v_F}u\ \ du\int_{|v-u|}^{|v+u|}dkk^4\sigma_{\mathrm{tr}}(k,v)\left[1+\frac{v^2-u^2}{k^2}\right]. \tag{3}$$

This expression takes into account the angular integration over the relative (electron-ion) velocities, here represented by k (with $\vec{k}=\vec{u}-\vec{v}$), and the integration of electron velocities u between 0 and v_F [22].

Here

$$\sigma_{\mathrm{tr}}(k,v)=\frac{4\pi}{k^2}\sum_{l=0}^{\infty}(l+1)\sin^2[\delta_l(k,v)-\delta_{l+1}(k,v)] \tag{4}$$

is the transport cross section corresponding to the scattering of electrons in the moving-ion potential. We note that σ_{tr} depends also on the ion velocity v due to the optimization of the scattering potential (through the adjustment of the screening parameter α) as described before [note that the phase shifts in Eq. (4) also depend on v].

We use this model to represent the contribution of valence electrons to the energy loss. So in the following we refer to this calculations as the *valence electron stopping power – extended sum rule* method (or VESP-ESR). This gives the main contribution to the stopping power for low and intermediate energies, including the stopping power maximum. However, with increasing energies the role of inner shells becomes also important. Then, in order to consider the application of this model to calculate the stopping power of solids in an extended energy range, we should include the additional contributions from the inner shells. There are various perturbative models which may be used in this case [7–9,27–29], however some of them use a first-order Born approximation and yield only the Z^2 term. A useful description for these contributions is the one given by the oscillator model [7–9] which allows us to evaluate the Z^2,Z^3, and Z^4 terms, in the stopping power expansion:

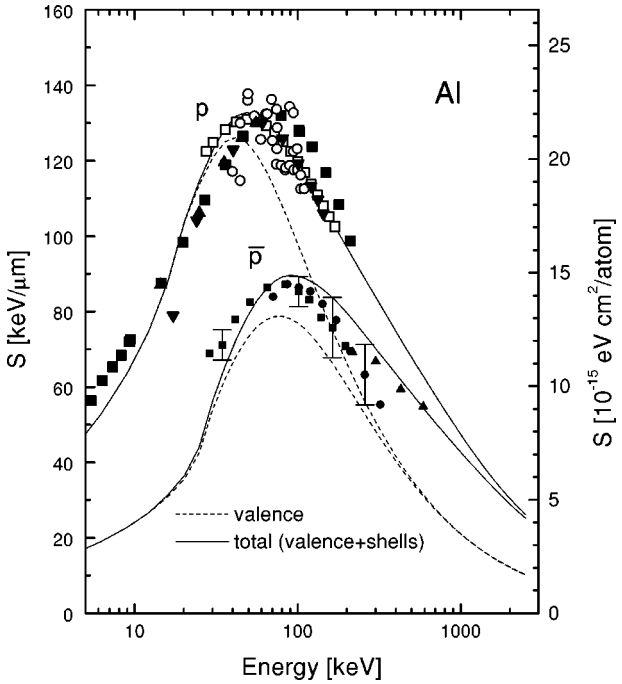

FIG. 1. Energy loss of protons and antiprotons in aluminum. The dashed lines show the contributions to the energy loss given by valence electrons, calculated according to the VESP-ESR model, while the solid lines show the total energy loss (including the inner-shell contributions). The points show the experimental results for protons (from Refs. [30–33]) and antiprotons (from Ref. [13]).

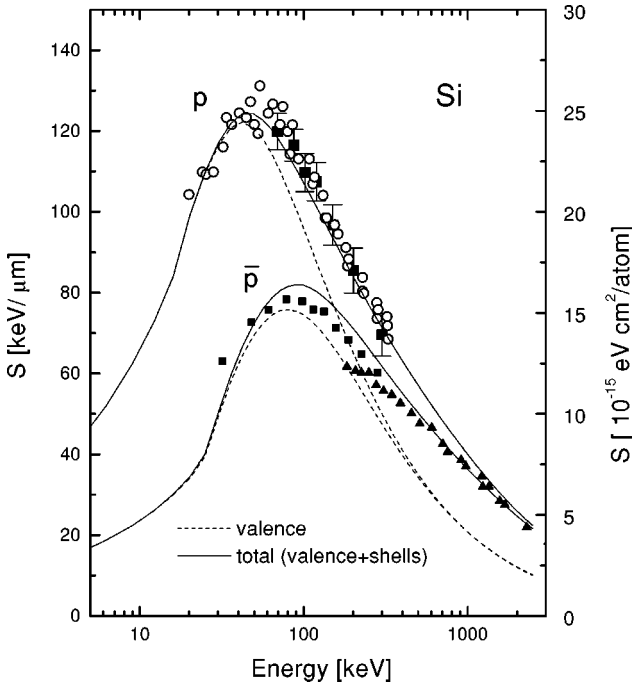

FIG. 2. Energy loss of protons and antiprotons in silicon. The dashed lines show the contributions to the energy loss given by valence electrons, calculated according to the VESP-ESR model, while the solid lines show the total energy loss (including the inner-shell contributions). The points show the experimental results for protons (from Refs. [34,35]) and antiprotons (from Ref. [13]).

$$S_{\text{inner shells}}=\frac{4\pi Z_2 n_a}{v^2}Z_1^2[L_0(v)+Z_1L_1(v)+Z_1^2L_2(v)], \tag{5}$$

where n_a is the atomic density of the solid. It is expected that this will yield the relevant terms of a convergent expansion for relatively large velocities, as long as $L_0(v)>Z_1L_1(v)>Z_1^2L_2(v)$. Therefore, the total stopping power will be calculated here by the sum of Eqs. (3) and (5), namely, $S_{\text{total}}=S_{\text{valence}}+S_{\text{inner shells}}$.

These calculations have been performed for the cases of protons and antiprotons in aluminum and silicon. These cases are of great interest due to the recently reported measurements by Møller *et al.* [13], these being the two elements where experimental data exist down to the lowest energies for antiprotons ($\sim$30 keV), and where the role of valence electrons is dominant. In the case of heavy targets the inner-shell corrections become more important as compared with the VESP-ESR results, and so the uncertainty of the calculations would probably increase.

III. RESULTS AND DISCUSSION

The results of these calculations are shown in Figs. 1 and 2, where we compare the results obtained from the present calculations with existing stopping power data for protons and antiprotons on a wide range of energies. The data for protons were taken from various sources [30–35], while those of antiprotons are taken from Ref. [13]. In each case we show with dashed lines the contribution to the stopping power due to valence electron (from the VESP-ESR model), and with solid lines the total stopping power values. We observe that the position and magnitude of the maxima predicted by the model are in good agreement with the experiments. As expected, we find that valence electrons play the dominant role in the stopping process for energies around the maximum.

We note also that the theoretical evaluations of stopping powers for antiprotons using the oscillator model for all the atomic shells, as given in Ref. [13], yield also very good results in the cases of aluminum and silicon. However, if the same model is used to calculate the corresponding values for protons (and using also the same shell parameters from Ref. [13]), one obtains values which are about 75% larger for Al and 50% large for Si, and the position of the maxima is displaced to lower energies.

On the other hand, the quadratic response model [14] is also unable to account quantitatively for the stopping power maximum in real targets [21]. Hence, the convenience of a fully nonlinear model to evaluate the energy loss due to valence electrons becomes evident.

We finally note that the present calculations for protons did not include the contribution of capture and loss processes in the intermediate range of energies. Calculations using first-order Born approximations for various processes [36] indicate that the corrections may be of about 10–15 % at $v\approx 1$. Other calculations by several authors [21,14,37] have disregarded or neglected this contribution. A precise evaluation of these effects in the intermediate range of velocities would deserve further study, although it lies beyond the scope of this paper. In any case, it is clear that the use of antiprotons provides the best probe for studying the energy loss phenomenon in the absence of any electron capture and

loss effect, and it may be the best way to test the theoretical models on nonlinear effects.

The present model gives a suitable estimation of the magnitude of the dynamical nonlinear effects on a wide range of energies. The calculations for p and $\bar{p}$ indicate that one should also expect important nonlinear effects for the slowing down of atomic ions in solids through the intermediate energy range. The application of this model may provide also a useful approach to the relevant question of describing the maximum of the stopping power curves for different ions.

In summary, we have shown that a consistent description of the Barkas effect in the range of intermediate energies, as expressed by the differences in the stopping power values for protons and antiprotons in solids, requires a study of dynamical nonlinear effects which cannot be well represented by the usual perturbative expansions. The VESP-ESR model presented here provides a self-consistent nonperturbative picture of the energy loss process and of the Barkas effect in the important energy range around the stopping maximum. The present model yields the contribution of valence electrons which dominate the stopping process at low and intermediate energies for light targets. The contributions from inner shells, which are increasingly important for energies above the stopping maximum, appear to be fairly well represented in the upper energy range by the atomic oscillator model.

ACKNOWLEDGMENTS

The authors gratefully acknowledge financial support from Consejo Nacional de Investigaciones Científicas y Técnicas (CONICET) and Fundación Antorchas, and useful discussions with J. E. Miraglia.

[1] W.H. Barkas, W. Birnbaum, and F.M. Smith, Phys. Rev. **101**, 778 (1956); W.H. Barkas, N.J. Dyer, and H.H. Heckman, Phys. Rev. Lett. **11**, 26 (1963).
[2] H. Bethe, Ann. Phys. (Leipzig) **5**, 325 (1930).
[3] J.C. Ashley, R.H. Ritchie, and W. Brandt, Bull. Am. Phys. Soc. **15**, 1338 (1970); Phys. Rev. B **5**, 2393 (1972).
[4] J.C. Ashley, R.H. Ritchie, and W. Brandt, Phys. Rev. A **8**, 2402 (1973); **10**, 737 (1974).
[5] J.D. Jackson and R.L. McCarthy, Phys. Rev. B **6**, 4133 (1972).
[6] K.W. Hill and E. Merzbacher, Phys. Rev. A **9**, 156 (1974).
[7] P. Sigmund and U. Haagerup, Phys. Rev. A **34**, 892 (1986).
[8] H.H. Mikkelsen and P. Sigmund, Phys. Rev. A **40**, 101 (1989).
[9] H.H. Mikkelsen, Nucl. Instrum. Methods Phys. Res. B **58**, 136 (1991).
[10] H. Bichsel, Phys. Rev. A **41**, 3642 (1990).
[11] L.H. Andersen, P. Hvelplund, H. Knudsen, S.P. Møller, J.O.P. Pedersen, E. Uggerhøj, K. Elsener, and E. Morenzoni, Phys. Rev. Lett. **62**, 1731 (1989); G. Gabrielse, X. Fei, L.A. Orozco, S.L. Rolston, R.L. Tjoelker, T.A. Trainor, J. Haas, H. Kalinowsky, and W. Kells, Phys. Rev. A **40**, 481 (1989); R. Medenwaldt, S.P. Møller, E. Uggerhøj, T. Worm, P. Hvelplund, H. Knudsen, K. Elsener, and E. Morenzoni, Nucl. Instrum. Methods Phys. Res. B **58**, 1 (1991).
[12] S.P. Møller, E. Uggerhøj, H. Bluhme H. Knudsen, U. Mikkelsen, K. Paludan, and E. Morenzoni, Nucl. Instrum. Methods Phys. Res. B **122**, 162 (1997).
[13] S.P. Møller, E. Uggerhøj, H. Bluhme, H. Knudsen, U. Mikkelsen, K. Paludan, and E. Morenzoni, Phys. Rev. A **56**, 2930 (1997).
[14] J.M. Pitarke, R.H. Ritchie, and P.M. Echenique, Phys. Rev. B **52**, 13 883 (1995).
[15] I. Nagy, A. Arnau, P.M. Echenique, and E. Zaremba, Phys. Rev. B **40**, 11 983 (1989).
[16] P.M. Echenique and M.E. Uranga, in *Interaction of Charged Particles with Solids and Surfaces*, Vol. 271 of *NATO Advanced Study Institute Series B: Physics*, edited by A. Gras-Martí, H.M. Urbassek, N. R. Arista, and F. Flores (Plenum, New York, 1990), p. 39.
[17] I. Nagy, B. Apagyi, and K. Ladànyi, Phys. Rev. A **42**, 1806 (1990).
[18] I. Nagy and P.M. Echenique, Phys. Rev. A **47**, 3050 (1993).
[19] I. Nagy, Nucl. Instrum. Methods Phys. Res. B **94**, 377 (1994).
[20] E. Zaremba, A. Arnau, and P.M. Echenique, Nucl. Instrum. Methods Phys. Res. B **96**, 619 (1995).
[21] I. Nagy and B. Apagyi, Phys. Rev. A **58**, R1653 (1998).
[22] A.F. Lifschitz and N.R. Arista, Phys. Rev. A **57**, 200 (1998).
[23] A.F. Lifschitz and N.R. Arista, Phys. Rev. A **58**, 2168 (1998).
[24] P. Sigmund, Nucl. Instrum. Methods Phys. Res. B **85**, 541 (1994).
[25] I. Nagy and A. Bergara, Nucl. Instrum. Methods Phys. Res. B **115**, 58 (1996).
[26] P. Sigmund, Phys. Rev. A **26**, 2497 (1982); L. De Ferrariis and N.R. Arista, *ibid.* **29**, 2145 (1984).
[27] J.R. Sabin and J. Oddershede, Phys. Rev. A **26**, 3209 (1982); **39**, 1033 (1989).
[28] D.E. Meltzer, J.R. Sabin, and S.B. Trickey, Phys. Rev. A **41**, 220 (1990).
[29] T. Kaneko, Phys. Status Solidi B **156**, 49 (1989); Research Report NIFS-DATA-9, National Institute for Fusion Science, Japan (1990).
[30] J.H. Ormrod and H.E. Duckworth, Can. J. Phys. **41**, 1424 (1963); J.H. Ormrod, J.R. Macdonald, and H.E. Duckworth, *ibid.* **43**, 275 (1965).
[31] W. White, J. Appl. Phys. **38**, 3660 (1967).
[32] S. Kreussler, C. Varelas, and R. Sizman, Phys. Rev. B **26**, 6099 (1982).
[33] C. Eppacher and D. Semrad, Nucl. Instrum. Methods Phys. Res. B **69**, 33 (1992).
[34] P. Mertens and P. Bauer, Nucl. Instrum. Methods Phys. Res. B **33**, 133 (1988).
[35] A. Ikeda, K. Sumitono, T. Nishioka, and Y. Kido, Nucl. Instrum. Methods Phys. Res. B **115**, 34 (1996).
[36] M. Peñalba, A. Arnau, P.M. Echenique, F. Flores, and R.H. Ritchie, Europhys. Lett. **19**, 45 (1992).
[37] N. Wang and I. Nagy, Phys. Rev. A **55**, 2083 (1997); N. Wang and J.M. Pitarke, *ibid.* **57**, 4053 (1998).